Dalton Transactions

An international journal of inorganic chemistry

www.rsc.org/dalton

Number 37 | 7 October 2009 | Pages 7561–7828

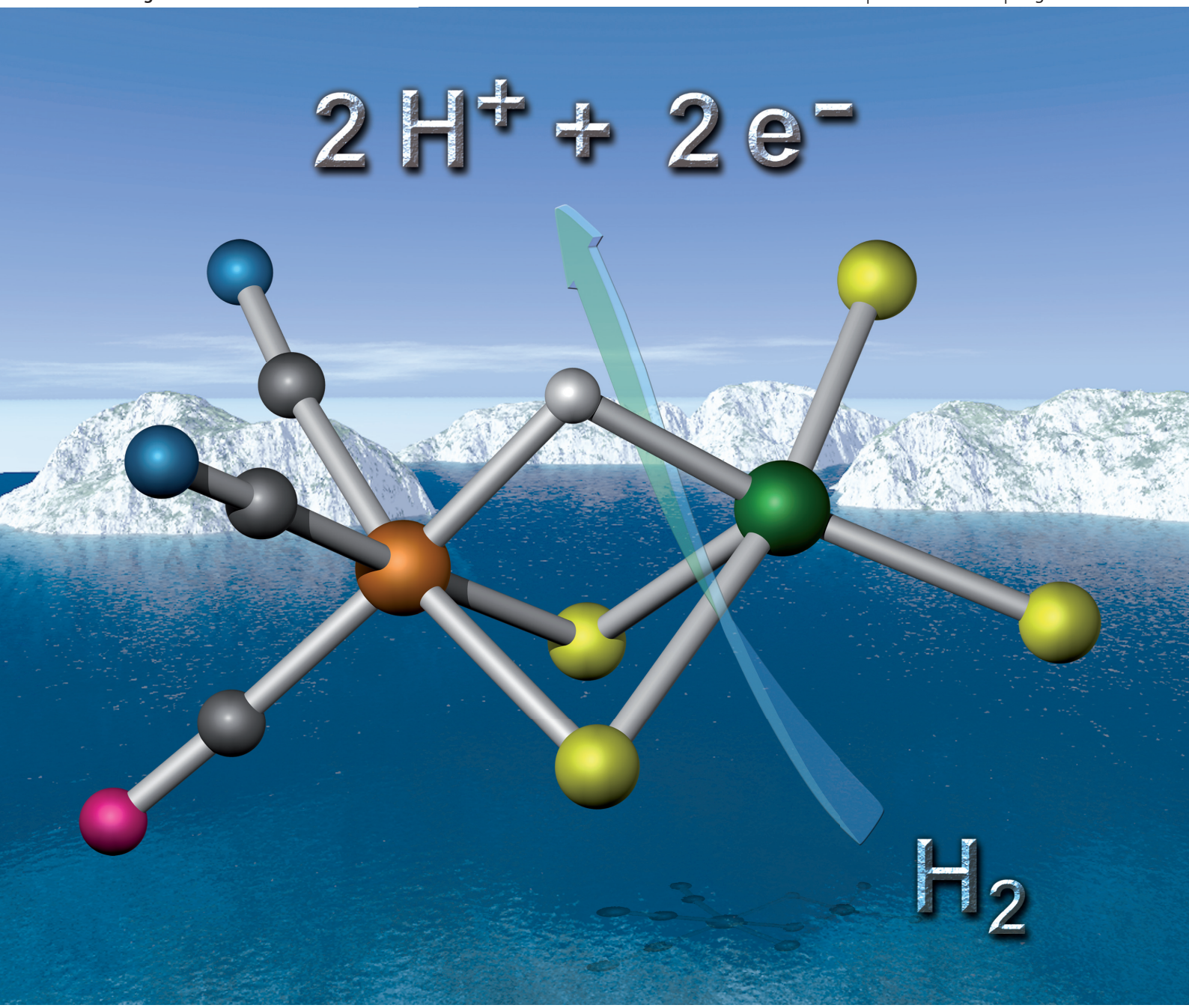

ISSN 1477-9226

RSC Publishing

1477-9226(2009)37;1-V

[NiFe] hydrogenases: structural and spectroscopic studies of the reaction mechanism

Hideaki Ogata,[a] Wolfgang Lubitz[a] and Yoshiki Higuchi*[b]

Received 26th February 2009, Accepted 19th May 2009
First published as an Advance Article on the web 2nd July 2009
DOI: 10.1039/b903840j

[NiFe] hydrogenases catalyze the reversible oxidation of dihydrogen. For this simple reaction the molecule has developed a complex catalytic mechanism, during which the enzyme passes through various redox states. The [NiFe] hydrogenase contains several metal centres, including the bimetallic Ni–Fe active site, iron–sulfur clusters and a Mg^{2+} ion. The Ni–Fe active site is located in the inner part of the protein molecule, therefore a number of pathways are involved in the catalytic reaction route. These consist of an electron transfer pathway, a proton transfer pathway and a gas-access channel. Over the last 10–15 years we have been investigating the crystal structures of the [NiFe] hydrogenase from *Desulfovibrio vulgaris* Miyazaki F, which is a sulfate-reducing anaerobic bacterium. So far the crystal structures of the oxidized, H_2-reduced and carbon monoxide inhibited states have been determined at high resolution and have revealed a rather unique structure of the hetero-bimetallic Ni–Fe active site. Furthermore, intensive spectroscopic studies have been performed on the enzyme. Based on the crystal structure, a water-soluble Ni–Ru complex has been synthesized as a functional model for the [NiFe] hydrogenases. The present review gives an overview of the catalytic reaction mechanism of the [NiFe] hydrogenases.

Introduction

Hydrogenases reversibly catalyze the simple chemical reaction:

$$H_2 \rightleftharpoons 2H^+ + 2e^-.$$

[a]*Max-Planck-Institut für Bioanorganische Chemie, Stiftstrasse 34-36, D-45470, Mülheim an der Ruhr, Germany*
[b]*Graduate School of Life Science, University of Hyogo, Koto 3-2-1, Ako-gun, Hyogo, 678-1297, Japan. E-mail: hig@sci.u-hyogo.ac.jp; Fax: +81 791 58 0177; Tel: +81 791 58 0179*

Hydrogenases are key enzymes, which play an important role in many microorganisms.[1] Such enzymes are interesting not only for basic research but also for future 'clean energy' applications since hydrogen is a sustainable and environmentally friendly energy source. Hydrogen production can be used as a biological energy source and dihydrogen consumption is useful for new types of fuel cells. Therefore, in the last few decades, great efforts have been made in order to understand the catalytic mechanism of hydrogenases.[2–7]

Hideaki Ogata

Hideaki Ogata obtained his PhD from Kyoto University in 2003 under the supervision of Prof. Y. Higuchi. He worked at Himeji Institute of Technology as a postdoc for half a year. Since 2003 he has been working at the Max-Planck Institut für Bioanorganische Chemie in Mülheim an der Ruhr, Germany as a postdoc under the supervision of Prof. Dr. W. Lubitz.

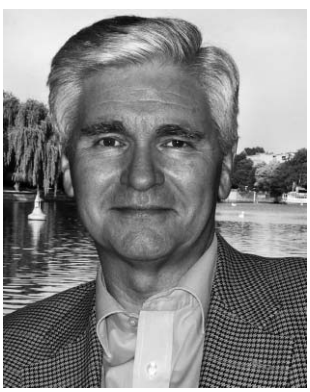

Wolfgang Lubitz

Wolfgang Lubitz received his doctorate and habilitation at the Freie Universität (FU) Berlin. He worked as a Max Kade Fellow at UC San Diego (1983–1984), as assistant and associate professor at the FU Berlin (1979–1989), as Professor at the Universität Stuttgart (1989–1991) and as a Full Professor at the Max Volmer Institute and Technische Universität Berlin (1991–2001). In 2000 he became a Scientific Member of the Max-Planck Society and Director at the Max-Planck Institute for Radiation Chemistry in Mülheim/Ruhr (later Max-Planck Institute for Bioinorganic Chemistry). He is an Honorary Professor at the Heinrich Heine Universität Düsseldorf. Since 2004 he is a member of the Council for the meetings of the Nobel Laureates in Lindau.

Hydrogenases can be categorized into three major classes according to the metal ions in their active site. The most studied class comprises the [NiFe] hydrogenases, which consist of a heteronuclear Ni–Fe active site coordinated further by cysteines and other organic/inorganic residues.[8,9] The sub-class of [NiFeSe] hydrogenases contains a selenocysteine instead of a cysteine bound to the Ni atom.[10] The second class comprises the [FeFe] hydrogenases, which consist of a dinuclear iron metal active site connected to an Fe_4S_4 cluster.[11–14] The third class comprises the [Fe] hydrogenases, formerly called iron–sulfur cluster-free hydrogenases or H_2-forming methylenetetrahydromethanopterin dehydrogenases (Hmd). These enzymes have a single Fe atom in their active site.[15–17]

The [NiFe] hydrogenase from *Desulfovibrio* (*D.*) *vulgaris* Miyazaki F is a periplasmic membrane attached enzyme. The overall structure of the [NiFe] hydrogenase is shown in Fig. 1B. The molecular mass of the enzyme is approximately 91 kDa and consists of two subunits. The large subunit has a molecular mass of about 62.5 kDa, while the small subunit has a molecular mass of 28.8 kDa. Spectroscopic results have shown that three iron sulfur clusters, one $[Fe_3S_4]^{1+/0}$ and two $[Fe_4S_4]^{2+/1+}$, are located in the small subunit. These are arranged in an almost linear fashion connecting the centre of the protein molecule to the molecular surface, the spacing between the centres is approximately 13 Å. The electrons provided by the heterolytic cleavage of dihydrogen at the Ni–Fe active site are transferred through this chain of Fe–S clusters to the physiological electron acceptor, cytochrome c_3.[18,19]

The active site of the [NiFe] hydrogenase from *Desulfovibrio sp.* is composed of one Ni and one Fe atom, which are bridged by two thiolates of cysteines (π-donors). Fig. 1A shows the active site of a standard [NiFe] hydrogenase in the oxidized form. The Fe^{2+} atom at the active site during the catalytic cycle remains low spin (S = 0) and does not change the oxidation state. Three diatomic non-protein ligands are bound to the Fe atom, which are assigned to two CN^- (σ-donors) and one CO (π-acceptor) based on Fourier transform infrared (FTIR) spectroscopic studies.[20] In the *D. vulgaris* Miyazaki F hydrogenase the two diatomic ligands are hydrogen bonded to the side-chain atoms of Arg479 (Arg463 in *D. gigas*) and Ser502 (Ser486 in *D. gigas*), respectively. On the other side the Ni atom is additionally coordinated by two more thiolates of cysteines bound in a terminal fashion. Between the various redox forms of the enzyme it is the Ni site that changes the oxidation state (*i.e.* Ni^{3+}, Ni^{2+} or even Ni^{1+}), and has therefore been proposed to be the site where cleavage of the dihydrogen occurs. Depending on the oxidation state of the enzyme a third bridging ligand between the two metals can be present.

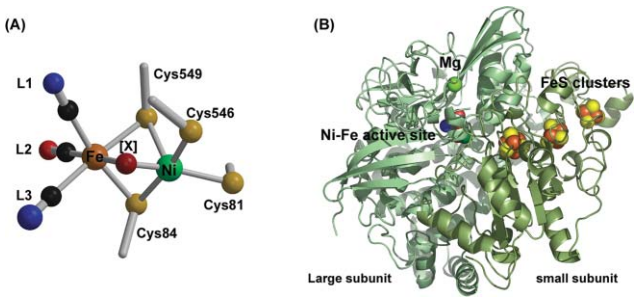

Fig. 1 Structure of the active site of the [NiFe] hydrogenase in the oxidized states (A). The third bridging ligand (X = oxygen/sulfur species) may be present depending on the oxidation state. The diatomic ligands, L1, L2 and L3 were assigned to CN^-/CO/SO, CO/CN^-, and CN^-/CO, respectively.[8,22,42,56] In the case of *D. vulgaris* Miyazaki F hydrogenase, the possibility of the SO ligand was also proposed at the L1 site.[8,92] The overall structure of the [NiFe] hydrogenase from *D. vulgaris* Miyazaki F (B).

A schematic diagram of the various redox states of the [NiFe] hydrogenase is shown in Fig. 2. The two most oxidized inactive states are known as Ni-A (unready) and Ni-B (ready). Both states are paramagnetic (Ni^{3+}, S = 1/2), but are distinguished by different *g*-values and activation rates. The Ni-B state is easily activated within a few minutes under hydrogen atmosphere, whereas the Ni-A state requires longer activation times of up to hours.[21]

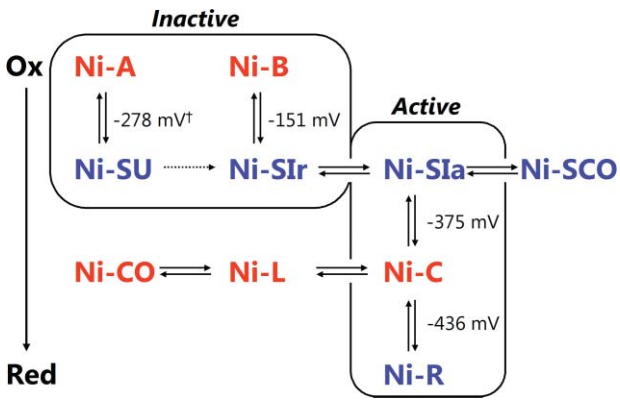

Fig. 2 Schematic representation of the various redox states of the [NiFe] hydrogenase. The EPR-detectable states and the EPR-silent states are shown in red and blue, respectively. The nomenclature of the states: Ni-A (unready state), Ni-B (ready state), Ni-SU (EPR-silent unready state), Ni-SIr (EPR-silent ready state), Ni-SIa (EPR-silent active state), Ni-SCO (EPR-silent CO inhibited state), Ni-C (EPR-detectable reduced state), Ni-L (Light induced state), Ni-CO (EPR-detectable CO inhibited state), and Ni-R (EPR-silent reduced state), respectively. The midpoint potentials measured for the [NiFe] hydrogense from *D. vulgaris* Miyazaki F at pH 7.4, 30 °C are shown against the standard hydrogen electrode.[25] The midpoint potential of the Ni-A and Ni-SU was measured at pH 8.4, 4 °C (Pandelia *et al.*, unpublished data).

Yoshiki Higuchi

Yoshiki Higuchi obtained his PhD from Osaka University (1984). After a postdoctoral position at Institute for Protein Research in Osaka University, he was appointed as an Assistant Professor at Himeji Institute of Technology (1985). He moved to Kyoto University in 1995 as an Associate Professor of Graduate School of Science. He received the Award of The Crystallographic Society of Japan in 1999. In 2002 he moved to Himeji Institute of Technology, to become a Professor in the Graduate School of Science. He is currently a Professor in the Graduate School of Life Science, University of Hyogo.

Recent crystallographic studies of the Ni-A and Ni-B states from *D. vulgaris* Miyazaki F, *D. gigas* and *D. fructosovorans* have revealed that the third bridging ligand present in the Ni-A and Ni-B states is different.[22,23] This distinct chemical identity of the third bridging ligand between these two states is thus proposed to be the origin of the different activation kinetics observed. When Ni-A and Ni-B states are one electron reduced, they give rise to EPR-silent states (Ni^{2+}), termed Ni-SU (EPR-silent unready) and Ni-SIr (EPR-silent inactive ready), respectively. These states are inactive and the bridging ligand probably still remains in the active site. The Ni-SIr state is subsequently activated by the release of the oxygenic species as water and forms the Ni-SIa (EPR-silent active) state which probably lacks the bridging ligand X (See Fig. 1A). Upon further one electron reduction of Ni-SIa, the paramagnetic state known as Ni-C (Ni^{3+}, $S = 1/2$) is reached. Ni-C is light sensitive and under illumination at cryogenic temperatures converts to a paramagnetic state named Ni-L. One electron reduction of Ni-C results in the most reduced states, called Ni-R. These states are EPR-silent (Ni^{2+}). Based on infrared studies up to three different Ni-R states have been observed.[24,25]

Up to now crystal structures have been determined for five [NiFe] hydrogenases found in sulfate-reducing bacteria (*D. vulgaris* Miyazaki F,[8] *D. gigas*,[9] *D. fructosovorans*,[23,26] *D. desulfuricans*,[27] *Desulfomicrobium baculatum*[10]). It was only until very recently that the first crystallographic results on the [NiFe] hydrogenase from a photosynthetic bacterium, *Allochromatium* (*A.*) *vinosum*, were reported.[28] In this review, we mainly focus on the crystallographic and spectroscopic studies of the [NiFe] hydrogenase from *D. vulgaris* Miyazaki F in its various oxidation states.

The oxidized states

The Ni-A state

The [NiFe] hydrogenases from sulfate-reducing bacteria are inactivated in the presence of oxygen. In view of the possible biotechnological applications of hydrogenases, it is thus important to obtain knowledge of the activation/inactivation processes. It has been shown that Ni-A does not directly react with H_2.[21] An electrochemical study further showed that when O_2 is added to the active enzyme under reducing conditions (0 mV *vs.* NHE) the enzyme formed mainly Ni-B. But in the case where O_2 is added at higher potentials (200 mV *vs.* NHE) most of the enzyme converted to the Ni-A state.[21,29,30] Interestingly the O_2-tolerant regulatory [NiFe] hydrogenase from *Ralstonia* (*R.*) *eutoropha* shows neither Ni-A nor Ni-B states.[31]

The X-ray crystal structure of the [NiFe] hydrogenase from *D. vulgaris* Miyazaki F in the Ni-A state has been reported at ultra-high resolution (1.04 Å).[22] The electron density map of the active site of the Ni-A state is shown in Fig. 3A. Despite the very high resolution diffraction data, it still remained difficult to uniquely identify the three intrinsic non-protein ligands (CO/CN^-) of the Fe atom, since the difference in the electron density of these ligands is very small. Therefore the exact coordination sites of CN^- and CO based solely on crystallographic results remains unclear. The distance between Ni and Fe atoms was found to be 2.80 Å. The electron density peak of the third bridging ligand site has a concave shape and suggests that this ligand is not a monatomic but a diatomic species. When this ligand was assigned to O_2, the O–O bond length became slightly longer (1.57 Å) than that of dioxygen compounds, such as O=O (1.2 Å) and hydrogen peroxide H_2O_2 (1.4 Å). In the Ni-A state, from *D. fructosovorans*, the electron density map also showed a diatomic ligand bound to the third bridging position.[23] In this work the third bridging ligand was assigned to a peroxide species (OOH^-). For the Ni-A state crystallographic experiments have shown an additional feature. The terminal cysteinyl residue Cys546 has an additional electron density peak on the sulfur, which is tentatively assigned to an oxygen species. The bridging Cys84 is also modified with a slightly weaker electron density peak, which is also assigned to an oxygen species (see Fig. 3A). Similar results for the [NiFe] hydrogenases from *D. fructosovorans* have been reported.[23] In *D. fructosovorans*, the crystal of the oxidized state was a mixture of the Ni-A and Ni-SU states. This was reflected in the electron density map of the crystal structure which also showed a similar modification in the sulfur of Cys75 (numbering *D. fructosovorans*, Cys84 *in D. vulgaris*) in the Ni-SU state. ^{17}O ENDOR experiments on the Ni-A state of the hydrogenase from *D. gigas* using $H_2{}^{17}O$ showed an oxygen based ligand bound to the Ni atom after a reduction/re-oxidation cycle.[32]

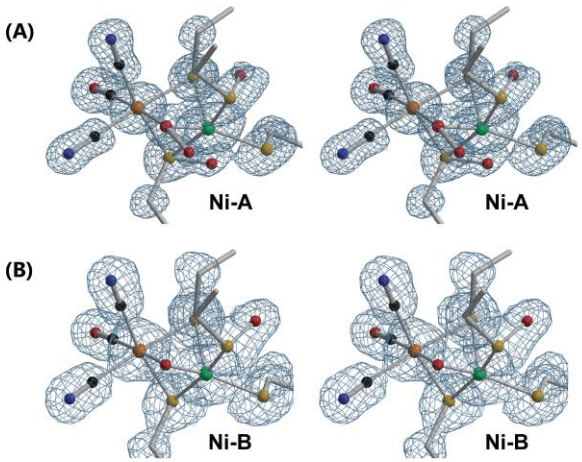

Fig. 3 Stereoview of the active sites of the Ni-A (A) and Ni-B (B) states, shown together with the electron density omit maps.[22]

However, from these experiments, the possibility of a sulfur based species at the position of the third bridging ligand cannot be excluded. Upon reduction with hydrogen using electron acceptors, such as methyl viologen (–448 mV), the oxidized enzyme liberates H_2S.[33] This indicates the possibility of a sulfur species near the active site. In fact, in the crystal structure analysis of the Ni-A state, when the oxygen species was assigned and refined at the bridging ligand site, a residual electron density remained around it, suggesting that some atomic species with more electrons, such as a sulfur species, may exist at the site. Further protein film voltammetry studies have shown that addition of Na_2S in the active state of the hydrogenase from *D. vulgaris* Miyazaki F at 0 mV (*vs.* NHE), resulted in a rapid deactivation of the enzyme. The activity could be recovered during a return sweep at 80mV *vs.* NHE.[34] When the active enzyme was exposed to O_2, it immediately became inactivated, while activity could be regained under a return sweep at –50 mV *vs.* NHE. An EPR

study on the reactions of *D. vulgaris* Miyazaki F hydrogenase with Na_2S showed that addition of Na_2S to the as-isolated enzyme under anaerobic conditions caused a rapid reduction of the Fe_3S_4 cluster. After exposure to atmospheric air, only the Ni-A state was obtained. These redox reactions can be well associated with the redox potential of Na_2S (–285 mV), which is comparable to those of the metal centres. The results suggest that Na_2S acts initially as a reductant and then as an inhibitor of the enzyme.[22,34] In the case of the Ru–Ge complexes, which also serve as a functional model of the hydrogenase, a hydroxo/sulfido bridge between the metals has been reported. These Ru–Ge complexes can activate dihydrogen heterolytically.[35,36] The sulfido Ru–Ge complex is less active and is activated slower than the hydroxo-bridged Ru–Ge complex (Matsumoto *et al.*, personal communication). This similarity of the different activation rates, which are observed in the case of the Ni-A and Ni-B states of the [NiFe] hydrogenase, could imply that a sulfur species may be present at the active site in the Ni-A state. Until now however, the exact assignment of the bridging ligand in the Ni-A state remains controversial.

The Ni-B state

After a purification procedure under aerobic conditions, the 'as isolated' enzyme shows EPR signals which are a mixture of the Ni-A ($g = 2.32, 2.24, 2.01$) and Ni-B ($g = 2.33, 2.16, 2.01$) states. The relative ratio of these states varies from each purification and in the case of *D. vulgaris* Miyazaki F hydrogenase the Ni-B state is dominant (around 70%). The g_x and g_z components of Ni-A and Ni-B states are very similar, but the g_y is significantly different. The direction of the g_y-axis points towards the direction of the third bridging ligand. For the crystallographic experiments, a pure Ni-B state was obtained by a H_2-reduction and O_2-re-oxidation cycle. The crystal structure of the Ni-B state was solved at 1.4 Å resolution.[22] The electron density map of the Ni-Fe active site in the Ni-B state is shown in Fig. 3B. The distance between the Ni and Fe atoms is slightly shorter (2.69 Å) than that of the Ni-A state (2.80 Å). The electron density peak of the third bridging ligand (X) is assigned to an monatomic oxygen species, most probably an OH^-.[22,37] A modification in the sulfur of Cys546 was also found and this was assigned to an extra oxygen species. The orientation of this atom was slightly different from the one found in the Ni-A state (see Fig. 3). No additional peaks were found at the active site.

In the first report of the crystal structure of the oxidized state from *D. vulgaris* Miyazaki F hydrogenase, the third bridging ligand was assigned to a sulfur atom since the crystallographic parameters of this electron density peak could not converge to an oxygen species.[8] In the case of the synthetic trinuclear Ni-Fe complex, $[NiSFe_2(CO)_6]$, which has a bridging sulfur between the Ni and Fe, the distance between the sulfur and Ni atoms was found to be 2.166 Å.[38] The same distance between the bridging sulfur and Ni atoms (2.16 Å in the oxidized state) was found in the *D. vulgaris* Miyazaki F hydrogenase.[8] Gas chromatography analysis of the Ni-B state indicated that H_2S was liberated when the as-isolated state and the Ni-B state were reduced by hydrogen and the amount of the liberated H_2S was in molar ratio to the enzyme of 0.24 and 0.08, respectively.[22] These results indicate that under natural conditions, or in the as-purified states, both oxygen and sulfur species can be bound to the Ni atom.[22,33,34]

A ^1H and ^2H hyperfine sub-level correlation spectroscopy (HYSCORE) of the Ni-B state in the *D. vulgaris* Miyazaki F hydrogenase was carried out in order to identify the third bridging ligand.[39] ^2H exchanged samples were prepared after the H_2O buffer was exchanged to D_2O subsequently followed by reduction with D_2 gas and re-oxidation with O_2. On the basis of a comparison of ^1H and ^2H HYSCORE spectra, one exchangeable proton was observed. It was assigned to the OH^- ligand at the third bridging position. This was confirmed by single crystal EPR and ENDOR spectroscopic studies.[37,40] These results suggested that the OH^- binds to the bridging position between Ni and Fe. From the results of the orientation dependent EPR and ENDOR spectra, the directions of the *g*-tensor and the hyperfine couplings were obtained.[37] The data showed that the OH^- lies approximately in the *xy*-plane of the spin-carring d_{z^2} orbital at the Ni. Results were in good agreement with DFT calculations on the magnitude and the orientation dependence of the hyperfine coupling constants attributed to the proton of the bridging ligand. Electron-Electron Double Resonance-Detected NMR (EDNMR) has been applied to the ^{61}Ni enriched Ni-B state and the spin population at ^{61}Ni was estimated to be 0.44.[41]

The reduced states (Ni-C/Ni-R)

After the enzyme enters the activation cycle through the EPR-silent state Ni-SIa, the valence of the Ni atom turns again to Ni^{3+} and shows an EPR-detectable state Ni-C with *g*-values at $g = 2.20, 2.14, 2.01$. An X-ray crystallographic analysis of the reduced state of [NiFe] hydrogenase from *D. vulgaris* Miyazaki F at 1.4 Å resolution revealed that the third bridging ligand had disappeared upon reduction with H_2.[42] A major difference in the active site between the oxidized and reduced states lies in the presence and absence of this third bridging ligand, respectively. In the reduced state the electron density peak between Ni and Fe was not present (see Fig. 4A). This suggests that the activation process requires removal of the oxygen–based bridging ligand prior to binding of the dihydrogen to the active centre where it can be subsequently cleaved. The distance between Ni and Fe in the active site becomes slightly shorter (2.55 Å) than that of the oxidized enzyme (2.80 Å in Ni-A, 2.69 Å in Ni-B, respectively). Some crystal structures of the reduced state showed a modification in the sulfur of the Cys546 terminal ligand. The orientation of this 'extra' species was similar to that of the Ni-B state (see Fig. 3B and 4A). An ^{17}O ENDOR study has also shown that the ENDOR signals found in the oxidized state were lost upon reduction to the Ni-C state.[32]

Since heterolytic cleavage of hydrogen takes place in the active site during the catalytic cycle, it has long been expected that a hydride would be bound at one of the metals or between the two metals. Direct experimental evidence for such a situation was obtained for the Ni-C state of the regulatory hydrogenase (RH) from *R. eutropha* by using ENDOR and HYSCORE spectroscopy. These studies have shown that a hydride is bound to the Ni atom in a direction approximately perpendicular to the *z*-axis of the Ni orbital, where the *z*-axis of the Ni atom is directed towards the sulfur of the Cys549 (see Fig. 4C).[43] A single crystal EPR and DFT studies for the Ni-C state of the hydrogenase from *D. vulgaris* Miyazaki F also showed that a hydride is binding the Ni and Fe atoms.[44] Additional orientation selected ENDOR and HYSCORE

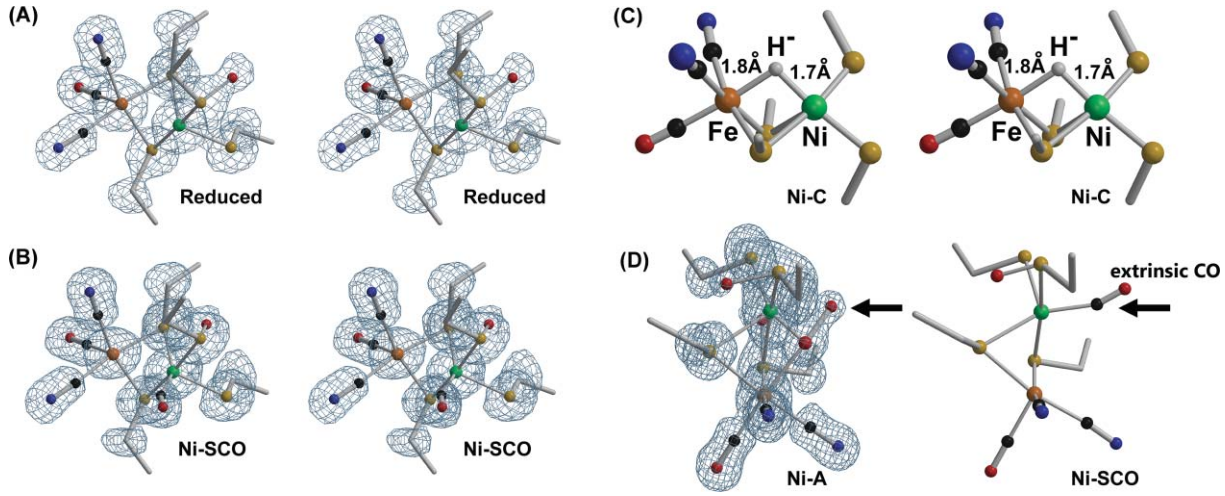

Fig. 4 Stereoview of the active site in the reduced state (A) and the CO-inhibited state (B).[42,56] Stereoview of the model of the Ni-C state from EPR spectroscopic analysis (C).[43] The ligand bridging the two metals in the Ni-C state was assigned to a hydride. The structure of the active site in the Ni-A state is shown with the electron density map (D left) and the structure of the Ni-SCO state (D right). The oxygen species of the third bridging ligand in the Ni-A state occupies the same position with the carbon atom of the extrinsic CO in the CO-inhibited state.[22,56]

studies have also uniquely identified the bridging hydride.[45] The major carriers of the spin density in the Ni-C state were found to be the Ni atom (~50%) and the sulfur of the Cys549.[46,47] This cysteine ligand carries a significant amount of spin density and makes a hydrogen bond to the His88.[48] Density functional theory calculations performed on these states gave results in good agreement with the observations.[49]

For the [NiFeSe] hydrogenase from *Desulfomicrobium baculatum*, another crystal structure of the reduced state has been reported at 2.15 Å resolution.[10] The electron density peak in the position of the third bridging ligand was also not observed. The distance between Ni and Fe atoms was found to be 2.5 Å, similar to that of the *D. vulgaris* Miyazaki F hydrogenase in the reduced state. The Glu23 residue (numbering *Desulfomicrobium baculatum*, Glu34 in *D. vulgaris*) forms a hydrogen bond to the selenocysteine Cys492 (Cys546 in *D. vulgaris*) and both exhibited relatively larger temperature factors compared to the rest of the active site. It has been postulated that the Cys546 and Glu34 are involved in the proton transfer process as will be described below.

Ni-C is light sensitive and upon illumination at cryogenic temperatures forms the Ni-L state. Ni-L can show two different forms (Ni-L1, $g = 2.30, 2.13, 2.05$ and Ni-L2, $g = 2.27, 2.12, 2.05$ in *D. gigas*), which are created by illumination at different temperatures.[50,51] When the enzyme in the Ni-C state from *D. vulgaris* Miyazaki F is illuminated below 100 K, the Ni-L1 state ($g = 2.30, 2.12, 2.05$) is obtained.[52] In the Ni-L state the hydride is proposed to be removed from the bridging position as a proton. This proton is accepted by a base nearby the active site, presumably by one of the sulfur atoms which coordinate the Ni. A wavelength dependent EPR study on the photo-conversion of Ni-C to Ni-L was carried out for the hydrogenase from *D. vulgaris* Miyazaki F. This study showed that this photo-conversion occurs in a broad range from 350 to 900 nm.[52] The action spectrum of the photoconversion *versus* the excitation wavelength λ showed peaks at 590 and 700 nm and a shoulder at 850 nm. These peaks indicate that the electronic transitions involve ligand based orbitals and only a small charge transfer character is present.

The CO-inhibited states (Ni-CO/Ni-SCO)

Carbon monoxide is known as a competitive inhibitor of the [NiFe] hydrogenase. Binding of CO to the active site can result in two distinct CO inhibited states, one that is paramagnetic (Ni-CO) and one that is EPR-silent (Ni-SCO). EPR spectroscopic analysis of the paramagnetic CO inhibited state of the *A. vinosum* hydrogenase using ^{13}CO showed that the extrinsic CO binds to the Ni atom.[53] The EPR-detectable Ni-CO state is described by lower g-values at $g = 2.13, 2.08, 2.02$ (in *D. vulgaris*) and is formed much slower than the EPR-silent Ni-SCO state.[54] The ^{13}CO hyperfine couplings and the *g*-values calculated by density functional calculations are in good agreement with the experimentally observed values, which suggest that CO binds in an axial position to a monovalent Ni^{1+}.[49] The Ni-CO state was shown to be light-sensitive upon illumination at cryogenic temperatures and converted to the same Ni-L state as Ni-C.[53]

Furthermore FTIR spectroscopic studies on the EPR-silent CO inhibited state from *A. vinosum* verified that the extrinsic CO is indeed bound to the active site.[55] Raman spectroscopy of this CO inhibited enzyme for *D. vulgaris* Miyazaki F showed an absorption band (430 cm^{-1}) when excited at 476.5 nm, which is assigned to a CO bound to Ni in a bent conformation.[56] Carbon monoxide does not bind to the Ni-A/SU and Ni-B/SIr states, but has the affinity to bind to the Ni-SIa state since the bridging ligand blocking the access of CO to Ni is absent in this state. Binding of CO to the Ni-SIa state therefore leads to the EPR-silent CO inhibited enzyme, whereas binding of CO to the Ni-L state leads to the paramagnetic CO inhibited state (see Fig. 2).

The high-resolution (1.2 Å) crystal structures of the Ni-SCO state of the [NiFe] hydrogenase from *D. vulgaris* Miyazaki F revealed that the extrinsic CO is bound to the Ni atom in a slightly bent conformation (see Fig. 4B).[56] The distance between Ni and the carbon atom of the extrinsic CO was 1.77 Å, while the Ni–C–O angles were approximately 160°. The distance between Ni and Fe was found to be 2.61 Å, which is slightly longer than that of the Ni-C state (2.55 Å). The Ni-SCO state is light sensitive.[55]

Upon illumination with white light at temperatures below 100 K, the extrinsic CO can be dissociated. In the dark state the extrinsic CO was not observed to be replaced by H_2. The electron density map, which calculated the difference between CO-bound and CO-liberated structures, exhibited a distinct change in the electronic distribution around Ni and the sulfur of the Cys546 residue. In the case of the [NiFeSe] hydrogenase this cysteinyl atom is coordinated to Ni in a terminal fashion, and is replaced by selenium. The temperature factor of this sulfur atom was larger than those of the other coordinating sulfur atoms in the active site. A number of crystal structures of the Ni-SCO state showed also an additional modification in the sulfur of Cys546. The orientation of this atom is similar to the one observed in the X-ray crystallographic studies of the Ni-A state (see Figs. 4B and 3A). It is noteworthy to mention that the Cys546 has been proposed to be the amino acid residue which receives the proton resulting from the dihydrogen cleavage.[57] This proton is further passed to the Glu34 residue, which is part of the proton transfer pathway (see below).

It was mentioned in the previous section that the bridging ligand of the Ni-A state was shown to be a diatomic species. The second atom of the third bridging ligand occupies the same position as the carbon atom of the extrinsic CO in the CO-inhibited state (see Fig. 4D). This suggests that the Ni-A state resembles the Ni-SCO state.[22,56,58] This observation is important as both states hinder the binding of molecular hydrogen to the empty coordination site of Ni.

When CO was introduced into a solution of the reduced [NiFe] hydrogenase, an analysis using the acetyl acetone method showed that formaldehyde (H_2CO) was present (Higuchi *et al.*, unpublished data). The amount of the detected formaldehyde was approximately equal to the enzyme in molar ratio. This result suggests that the CO is protonated at the carbon. The bent conformation of the Ni-SCO state found in *D. vulgaris* Miyazaki F hydrogenase, would also support this protonated carbon.[56]

The FeS clusters

The FeS clusters transport the electrons, which are produced by heterolytic cleavage of the dihydrogen at the active site, from the Ni-Fe active site to the molecular surface. In the case of the standard [NiFe] hydrogenases, three FeS clusters are found in the small subunit. The crystal structures from *D. vulgaris* and *D. gigas* hydrogenases showed one Fe_3S_4 cluster and two Fe_4S_4 clusters, which are situated almost linearly with distances between them of about 13 Å (see Fig. 5). The Fe_3S_4 centre is located in the middle of the electron transfer chain (medial cluster) of the FeS clusters. The distal Fe_4S_4 cluster is located near the surface of the protein. This cluster is held to the protein backbone by one His residue and three cysteines. The distance between the Ni-Fe active site and the proximal Fe_4S_4 cluster is 12 Å and only two cysteines are placed between them. Each cluster has different redox potentials that can affect the activity of the enzyme. In the case of hydrogenase from *D. gigas* the medial Fe_3S_4 cluster has a higher redox potential (–70mV) than that of the Fe_4S_4 clusters (–290 mV and –340 mV).[59] For the [NiFe] hydrogenase from *D. vulgaris* Miyazaki F the structural properties of this medial high potential cluster were further studied by high field (94GHz) EPR spectroscopy. Two different forms of the $[Fe_3S_4]^{+1}$ cluster were observed, which were pH-dependent. The *g*-tensors and hyperfine-tensors were further

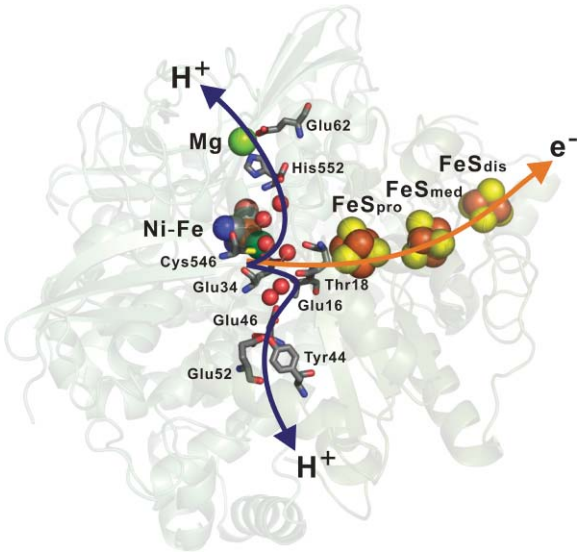

Fig. 5 Electron transfer chain (shown by the orange arrow) and possible proton transfer pathways (shown by the blue arrows).

determined using spectroscopy of a single crystal (g = 2.0258, 2.0174, 2.0110).[60]

In the photosynthetic bacterium *A. vinosum* one of the Fe_4S_4 clusters is suggested to convert to an Fe_3S_x cluster when the enzyme is reduced and re-oxidized.[61] On the other hand the [NiFeSe] hydrogenases exhibits more complicated features in their small subunit and have been shown to have only Fe_4S_4 clusters. In the F_{420}-reducing [NiFeSe] hydrogenase from *Methanococcus voltae*, conversion of the medial Fe_4S_4 to a Fe_3S_4 cluster by site directed mutagenesis was verified by an increase in the redox potential of this cluster by about 400 mV. However the activity of the mutated enzyme did not change when benzyl viologen (–350 mV) was used as an electron acceptor, but the activity was decreased 10-fold when the natural electron acceptor F_{420} (–360 mV) was used.[62] A conversion of the medial Fe_3S_4 to an Fe_4S_4 cluster was achieved by site-directed mutagenesis (P238C) in the *D. fructosovorans* [NiFe] hydrogenase (Pro242 in *D. vulgaris*), with a proline occupying the fourth empty position of the Fe site of the cluster. In this study it was shown that the midpoint potential of the Fe_3S_4 cluster dropped from +65 mV to –250 mV and the H/D exchange activity was slightly decreased.[63] It has been assumed that the electron transfer *via* the high redox-potential Fe_3S_4 cluster is unfavourable from a thermodynamic point of view. The H/D exchange reaction does not relate directly to the electron transfer process. However the conversion of the Fe_3S_4 to the Fe_4S_4 cluster showed less activity and this suggests that the Fe_3S_4 cluster is crucial for the electron transfer.

C-terminus Mg site and proton pathways

In the C-terminus region of the [NiFe] hydrogenase from *D. vulgaris* Miyazaki F, a Mg^{2+} atom is coordinated to the C-terminal His552 of the large subunit (see Fig. 6).[8] The other [NiFe] hydrogenases from *Desulfovibrio* species showed a similar coordination, but the [NiFeSe] hydrogenase from *Desulfomicrobium baculatum* has an Fe atom instead of Mg.[10] This Mg ion forms a distorted octahedral coordination and binds to the Glu62, His552, to the

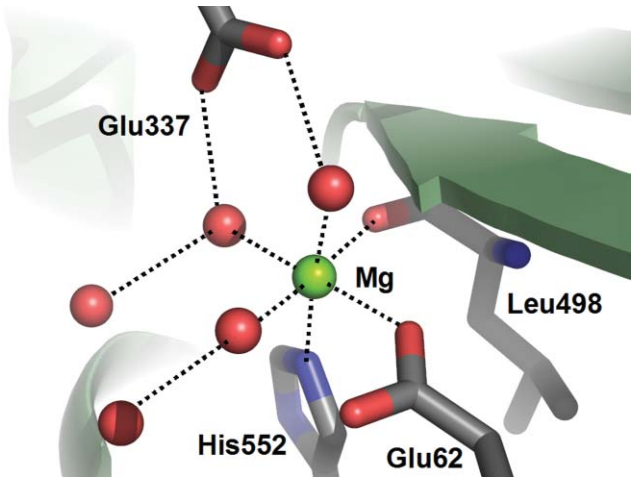

Fig. 6 C-terminus Mg site.[8] The Mg ion is shown with a light green sphere. The water molecules are represented by red spheres. The bonds to the Mg atom and the hydrogen bonds are represented by the dotted lines.

backbone of Leu498, and to three water molecules (in *D. vulgaris*). The binding of these amino acids is well conserved except for leucine, since it coordinates to the Mg using the O atom of the peptide bond. The three water molecules form hydrogen bonds to Gln497, Glu337 and other water molecules, respectively. It is believed that the Mg metal is involved in the maturation process since 15 amino acids of the C-terminus of the precursor were digested at the position of His552 in the maturation of the enzyme. The role of the Mg atom is probably to stabilize the C-terminal region, which is not exposed directly to the solvent region. However, a final conclusion on the role of this metal is still not available.

The Mg binding site is located near the active site within a distance of ~13 Å. A hydrogen bonding network, which is considered as the proton transfer pathway, is found between the Mg and the Ni-Fe active site. In the case of the *D. vulgaris* Miyazaki F hydrogenase this pathway is composed of two histidines, one of which is the C-terminus His552, two glutamate residues (Glu34 and Glu62) and several water molecules (see Fig. 5). In the *D. gigas* hydrogenase a similar pathway has been found and is composed of four histidines, one glutamate and several water molecules. Recently another possibility for the proton pathway has been suggested.[64] A theoretical study using Monte Carlo and Poisson-Boltzmann methods applied to the *D. gigas* hydrogenase indicated another possible proton pathway involving Glu18, His20, His13, Glu16, Tyr44, Glu46, Glu57, Glu73 (Glu 34, His36, His13, Glu16, Tyr44, Glu46, Glu57, Glu75 in *D. vulgaris*) and several water molecules which are placed near the proximal cluster.[64] Similar proton pathways could be found on the basis of a distance-based hydrogen bonding network analysis in the hydrogenase from *D. vulgaris* Miyazaki F. One pathway contains, for example Glu34, Thr18, Glu16, Glu46, Tyr44, Glu52 and several water molecules (see Fig. 5) (Ogata *et al.*, unpublished data). In *D. fructosovorans*, similar pathways were also obtained by QM/MM studies.[65] In all of the possible pathways proposed, the Cys546 and Glu34 residues (*D. vulgaris* numbering) form the initial part of the proton transfer pathways. The [NiFe] hydrogenase from *D. fructosovorans* in which the Glu25 (*D. fructosovorans* numbering, Glu18 in *D. gigas*, Glu34 in *D. vulgaris*) was mutated to a Gln, did not show catalytic activity. On the other hand the E25D mutant exhibited a para-H_2/ortho-H_2 conversion[66], whereas a decrease in the hydrogen isotope exchange activity was observed.[57] These results indicate that the proton is transferred *via* the hydrogen bonding network involving the Glu34 residue, which appears to be essential for the proton transfer.

The hydrophobic gas-access channel

The active site of the [NiFe] hydrogenase is buried in the centre of the enzyme, which suggests that a gas-access channel exists between the solvent accessible surface and the active site. Hydrogen (H_2) and other molecules such as O_2, CO can access the active site through this hydrophobic gas-access channel. It is known that Xe binds to the hydrophobic part of the protein and has been used as a probe of the hydrophobic gas-access channel. The crystal structure of the Xe-bound hydrogenase from *D. vulgaris* Miyazaki F has been solved at 1.8 Å resolution (Ogata *et al.*, unpublished data). Electron density peaks of Xe atoms were observed in the hydrophobic surrounding of the amino acid residues in the molecule. The crystal structure of the Xe-bound [NiFe] hydrogenase from *D. fructosovorans* solved at 6.0 Å resolution and a molecular dynamics calculation have shown a small cavity that could reach the active site *via* several channels.[26] This study indicated that there are several channel entrances near the surface of the enzyme, which combine to one small channel leading to the active site. Calculation of the gas-access channel using a sphere of 1.0 Å radius suggested that the channel ends near the Ni atom of the active site. A similar cavity has been calculated for the *D. vulgaris* Miyazaki F hydrogenase, which was found to connect the active site to the molecular surface (see Fig. 7).

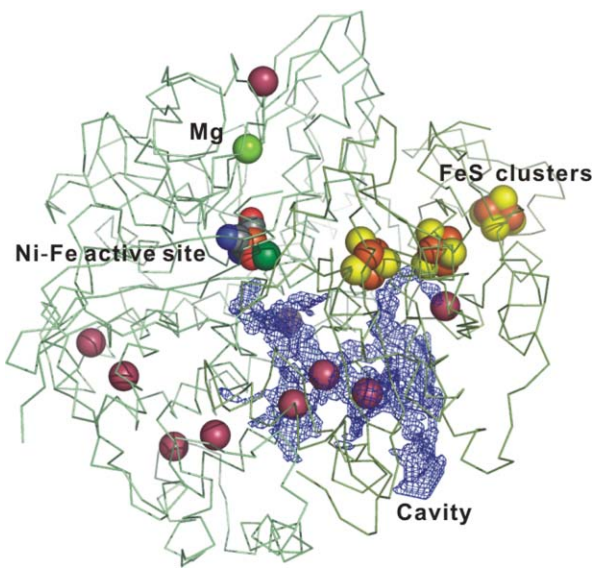

Fig. 7 Hydrophobic gas-access channel. Ten Xe atoms are observed by X-ray crystallography of high-pressured Xe-bound [NiFe] hydrogenase from *D. vulgaris* Miyazaki F. The blue map shows one of the calculated cavities that reaches to the active site from the molecular surface. Xe, Ni, Fe and Mg atoms are represented by magenta, dark green, orange and light green, respectively. The map of the cavity was calculated by Voidoo.

The standard [NiFe] hydrogenases are known as the oxygen-sensitive enzymes. It has been suggested that one of the reasons

for this sensitivity to O_2 depends on the size of the gas-access channel. In accordance no carbon monoxide inhibited state was observed in the case of the oxygen-tolerant H_2-sensing regulatory [NiFe] hydrogenase from *R. eutropha*.[67] For the regulatory [NiFe] hydrogenase from *R. eutropha* the double mutations of Phe and Ile to Leu and Val, which are located near the end of the gas-access channel, resulted in an increase of the size of the gas-access gate. These mutants exhibited oxygen sensitivity.[68] In the case of the membrane-bound [NiFe] hydrogenase from *R. eutropha*, a double mutant V77I + L125F (V83 and L131 in *D. vulgaris*) shows a decrease in oxygen sensitivity.[69] Recent crystallographic and spectroscopic studies on double mutants of the [NiFe] hydrogenase from *D. fructosovorans* (L122M + V74M, and L122F + V74I) (L131, V83 in *D. vulgaris*) showed that these mutations affect the gas-diffusion rate, with H_2 and CO.[70] CO binding and release rates for the L122M + V74M mutant are slower than those of the wild type.

To summarize the 'O_2-sensitivity/O_2-tolerance' of the hydrogenase might depend on several facts.[71] (1) The gas-accessibility: the environment of the gas-access channel affects the gas-diffusion rate.[70] (2) The reaction of O_2 with the active site: the binding of the O_2/CO (the inhibitors) takes place at the Ni atom. In the case of the O_2-tolerant soluble hydrogenase from *R. eutropha* it was proposed that a cyanide bound to the Ni prevent the direct O_2 access to the active site.[72,73] It has further been proposed that in O_2-tolerant hydrogenases an additional electron donor exists which provides extra electrons, which are required for a complete reduction of O_2 to water.[71] This donor still needs to be identified. (3) The recovery of the active state: the standard hydrogenases have oxygen-inhibited inactive states (the Ni-A and Ni-B states), which exhibit different activation rates. Fast recovery to the active state is required for the hydrogen oxidation under aerobic conditions.[74] In fact, no Ni-A state has been found for the O_2-tolerant hydrogenases.

Ni-Ru complexes

Since the first crystal structures of the active site of [NiFe] hydrogenases were determined, many hydrogenase models have been synthesized and investigated.[75–84] These have a mono- or bi-metallic site, such as Ni, Ni–Ni, Ni–Ru complexes that are active in an organic solvent. More recently, water-soluble Ni–Ru complexes have been synthesized; $[(Ni^{II}L)\ Ru^{II}(H_2O)\ (\eta^6\text{-}C_6Me_6)](NO_3)_2$ = $[1](NO_3)_2$, where L = N,N′-dimethyl-N,N′-bis(2-mercaptoethyl)-1,3-propanediamine.[85] Complex [**1**] has a water molecule bound to the Ru atom (see Fig. 8). In the Ni–Ru complex $[(Ni^{II}L)(H_2O)(\mu\text{-}H)Ru^{II}(\eta^6\text{-}C_6Me_6)](NO_3)$ = [**2**](NO_3), which was synthesized by the reaction of [**1**] with H_2 under ambient conditions (20 °C, 0.1 MPa H_2) in water, a μ-H^- bridging ligand was observed by neutron diffraction. The Ni–Ru distance (2.74 Å) of the complex [**2**] is significantly shorter than that of complex [**1**] (3.16 Å). A similar trend has been observed in the crystal structures of the native [NiFe] hydrogenases; in the Ni–Fe distances of the oxidized and the reduced state were 2.69–2.80 Å and 2.55 Å, respectively.[22,42]

The pH-dependent hydrogen isotope exchange reactions between gaseous isotopes (H_2, HD, D_2) and medium isotopes (H^+, D^+) have been investigated for the Ni–Ru complex (see Fig. 8). At pH between 4 and 6 the complex [**2**] catalyzed the isotope exchange reaction. However at pH between 7 and 10 hydrogenation of carbonyl compounds was catalyzed by the complex [**4**].[86] The complex [**1**] in the presense of H_2 reacted with $CuSO_4{\cdot}5H_2O$ in D_2O; consumption of H_2 and generation of HD and D_2 together with a two-electron reduction of Cu^{2+} were observed. In the hydrogen isotope exchange reaction of the Ni–Ru complex, the generation of HD and D_2 is simultaneous and pH-dependent, suggesting that there are two exchangeable proton species at the active site ([A] and [B] in Fig. 8).[87] A similar H/D exchange reaction has been observed in *D. vulgaris* Miyazaki F hydrogenase.[66] A catalytic mechanism for the Ni–Ru complex has

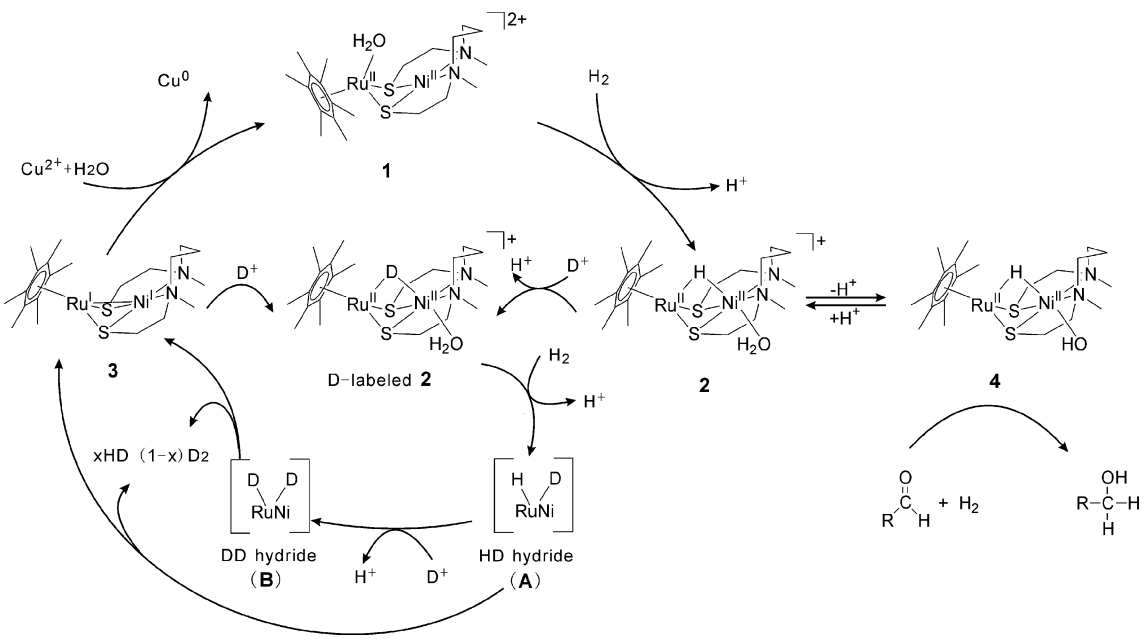

Fig. 8 The proposed catalytic reaction mechanism of the water-soluble Ni–Ru complex.[85–87]

been proposed (see Fig. 8) and it is suggested that the heterolytic cleavage of dihydrogen occurs twice during the reaction cycle.[87]

The first heterolytic activation of hydrogen with complex [**1**] leads to complex [**2**] with a μ-H^- bridge between Ni^{II} and Ru^{II}. The second heterolytic activation involves a dihydride species. When a D-labelled complex [**2**] reacts with H_2, the intermediate states [A]/[B] with HD/D_2 ligands is formed (see Fig. 8). The HD/D_2 is released simultaneously and the complex [**3**] is subsequently formed. Two electrons produced by the heterolytic cleavage of the hydrogen are used for the reduction of Cu^{2+} to Cu^0, and the complex [**3**] turns back to the initial state of the complex [**1**].

Catalytic reaction mechanism

In the process of the catalytic reaction, the [NiFe] hydrogenases pass through a number of redox states. In the past several reaction mechanisms have been proposed.[49,71,88–91] Here we want to discuss a slightly different mechanism that in based on the model studies. The proposed catalytic reaction mechanism is shown in Fig. 9. During the catalytic reaction process, the Fe^{2+} in the active site does not change the oxidation state. The most oxidized states Ni-A and Ni-B (both Ni^{3+}) are paramagnetic (S = 1/2) and distinguished by their *g*-values (EPR) and activation kinetics. The distinct difference between Ni-A and Ni-B lies in the identity of the third bridging ligand. In the Ni-B state, a hydroxide (OH^-) is bridging between the Ni and Fe metals. In the Ni-A state, a peroxide species has been discussed for the bridging position. One of the oxygen atoms of the bridging ligand in the Ni-A state occupies the same position as the CO inhibiting molecule, which binds to the sixth coordination site of Ni. This situation could provide the reason behind the difficulty to activate the Ni-A state compared to the Ni-B state, as Ni-A appears not to directly react with hydrogen. One-electron reduction of the fully oxidized Ni-A and Ni-B states leads to the EPR-silent Ni-SU and Ni-SIr states (both Ni^{2+}), respectively. Most probably the third bridging ligand is still retained in these states. The inactive states have the bridging ligand at the active site, therefore, the removal of the bridging ligand is necessary to activate the enzyme. In fact, the Ni-SIr state is activated by releasing the bridging ligand as a water molecule and forming the EPR-silent active Ni-SIa state (Ni^{2+}). The reaction

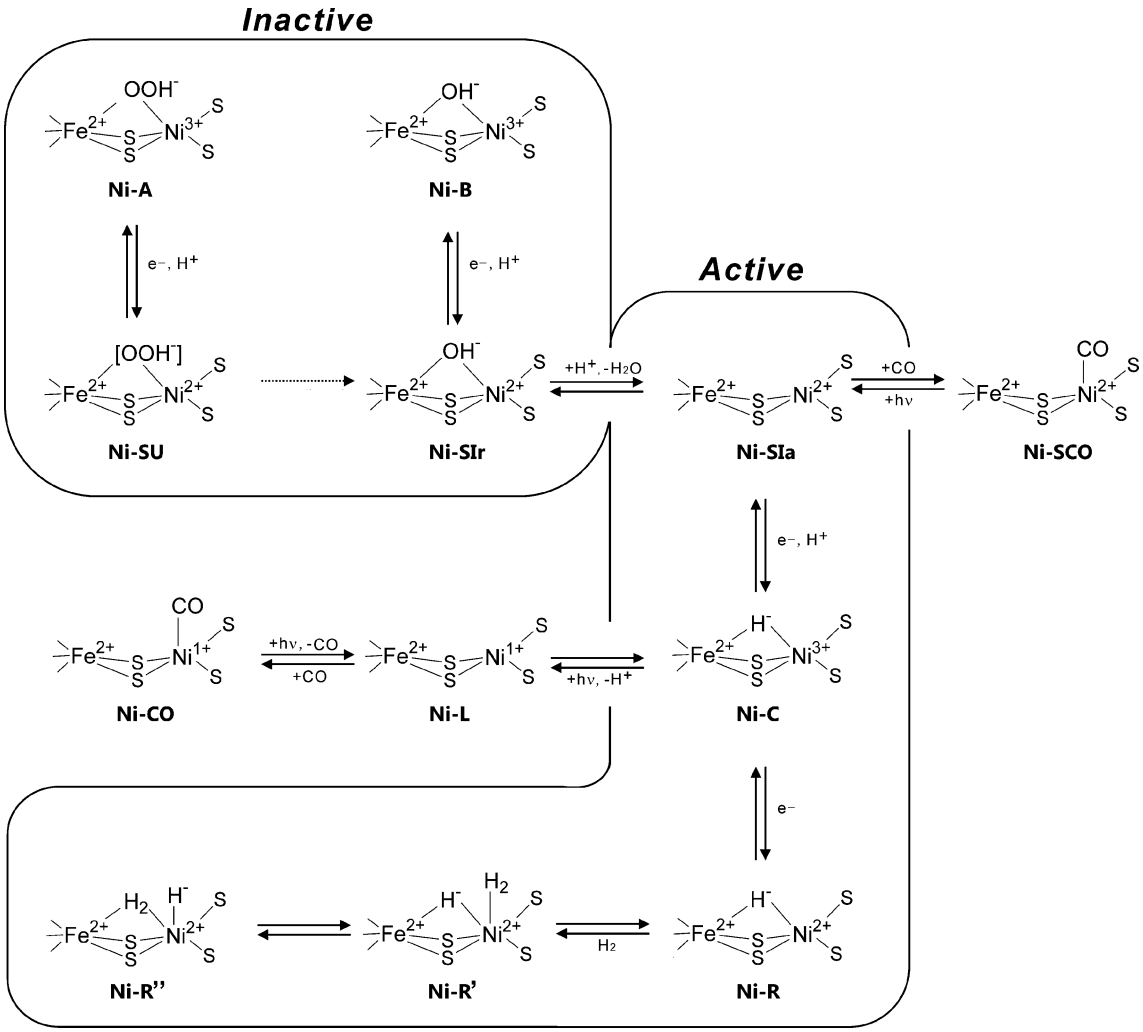

Fig. 9 Proposed enzyme activation, inhibition (by CO), light-sensitivity and a possible catalytic reaction mechanism of [NiFe] hydrogenase. In the Ni-A and the Ni-SU state the bridging ligand is tentatively assigned to OOH^-. The catalytic cycle could involve different Ni-R states; three possible states are given here. Release of H^- and an electron from the Ni-R″ generates Ni-C. A direct conversion from Ni-R″ or Ni-R′ to Ni-SIa is also possible, involving another H^+.

of O_2 with the Ni-SIa state leads to the inactive states (the Ni-A and the Ni-B states). Under anaerobic oxidation the Ni-B state is obtained. The Ni-SIa state can be inhibited by CO (EPR-silent Ni-SCO state), which binds to the Ni in a bent conformation. Upon illumination at cryogenic temperature, the Ni-SCO converts back to the Ni-SIa state. One electron reduction of the Ni-SIa state rapidly forms the paramagnetic Ni-C state (Ni^{3+}, $S = 1/2$). EPR spectroscopic studies clearly showed that in this state a hydride (H^-) forms a bridge between the Ni and Fe atoms. It is thus shown that in the catalytic active state of [NiFe] hydrogenase a μ-H^- species is bridging between the metals and the heterolytic hydrogen cleavage takes place at the active site. A similar coordination of the hydride bridge has been observed in the Ni-Ru complex by neutron diffraction experiments. The Ni-C state is light sensitive and at cryogenic temperature upon illumination with white light it reversibly converts to the paramagnetic Ni-L state (formerly Ni^{1+}). In the Ni-L state the hydride has been removed from the bridging position and probably moves as a proton to a base nearby the active site (reductive elimination). The inhibitor CO can bind to the Ni-L state and forms the EPR-detectable Ni-CO state (Ni^{1+}). The most reduced state of the catalytic cycle is termed Ni-R and is EPR-silent (Ni^{2+}). Up to three different Ni-R states have been observed by FTIR spectroscopy and have been shown to be pH dependent. This pH dependence indicates that the Ni-R states differ in the degree of protonation of the active site. H/D isotope exchange experiments in the reduced state have shown that the H/D exchange is observed in both the [NiFe] hydrogenase and the Ni-Ru complex. In the catalytic cycle of a Ni-Ru complex it is proposed that a dihydride species is formed. This suggests that during the catalytic cycle of the [NiFe] hydrogenase the hydrogen could be bound to the active site in several ways. In Fig. 9 possible structures for the different reduced states are shown with hydrogen and hydride bound to the nickel.

Conclusions

X-Ray crystallography, electron paramagnetic resonance (EPR) and other spectroscopic methods such as FTIR were applied to elucidate the structural, geometrical and electronic properties of the [NiFe] hydrogenase in the various redox states participating in the catalytic cycle. An extensive X-ray crystallographic analysis has been carried out on the Ni-A, Ni-B, Ni-SCO and the reduced (Ni-C/Ni-R) states. The results have shown conformational changes of the active site among the various physiologically relevant and exogenously inhibited states. All the paramagnetic states have been investigated by EPR spectroscopy, which enabled a characterization of the electronic structure of the active site and identification of the bridging ligands. There are still some open questions concerning a correct assignment of the active site species and the final reaction mechanism even though much effort has been dedicated to this problem over for many years. To address these questions, further investigations are necessary, especially isotope labelled EPR and FTIR spectroscopic studies, a structural analysis of the O_2-tolerant hydrogenases, and neutron diffraction experiments on single crystals of the [NiFe] hydrogenases. In addition, it was proposed that the hydrogenase could consume two dihydrogen molecules and produce two electrons, two protons and one new dihydrogen in one catalytic cycle.[87] A validation of this proposal is not easy but it would be important for understanding the catalytic mechanism of the enzyme.

Acknowledgements

We are grateful to Prof. T. Yagi, Prof. N. Yasuoka, Prof. S. Hirota and Prof. S. Ogo for fruitful collaborations. We thank M. E. Pandelia and L. J. Currell (MPI Mülheim) for helpful discussions and critically reading the manuscript. The work was supported by the GCOE Program (YH), the Japanese Aerospace Exploration Agency Project (YH), a Grant-in-Aid for Scientific Research (18GS0207) (YH), the basic research programs CREST type, "Development of the Foundation for Nano-Interface Technology" from JST, Japan (YH), the EU (Solar-H2) and the Max Planck Society.

References

1 P. M. Vignais and B. Billoud, *Chem. Rev.*, 2007, **107**, 4206.
2 S. P. J. Albracht, *Biochim. Biophys. Acta*, 1994, **1188**, 167.
3 A. L. De Lacey, V. M. Fernández, M. Rousset and R. Cammack, *Chem. Rev.*, 2007, **107**, 4304.
4 J. C. Fontecilla-Camps, A. Volbeda, C. Cavazza and Y. Nicolet, *Chem. Rev.*, 2007, **107**, 4273.
5 W. Lubitz, E. Reijerse and M. van Gastel, *Chem. Rev.*, 2007, **107**, 4331.
6 P. E. M. Siegbahn, J. W. Tye and M. B. Hall, *Chem. Rev.*, 2007, **107**, 4414.
7 K. A. Vincent, A. Parkin and F. A. Armstrong, *Chem. Rev.*, 2007, **107**, 4366.
8 Y. Higuchi, T. Yagi and N. Yasuoka, *Structure*, 1997, **5**, 1671.
9 A. Volbeda, M. H. Charon, C. Piras, E. C. Hatchikian, M. Frey and J. C. Fontecilla-Camps, *Nature*, 1995, **373**, 580.
10 E. Garcin, X. Vernede, E. C. Hatchikian, A. Volbeda, M. Frey and J. C. Fontecilla-Camps, *Structure*, 1999, **7**, 557.
11 J. W. Peters, W. N. Lanzilotta, B. J. Lemon and L. C. Seefeldt, *Science*, 1998, **282**, 1853.
12 B. J. Lemon and J. W. Peters, *Biochemistry*, 1999, **38**, 12969.
13 Y. Nicolet, C. Piras, P. Legrand, C. E. Hatchikian and J. C. Fontecilla-Camps, *Structure with Folding & Design*, 1999, **7**, 13.
14 Y. Nicolet, A. L. De Lacey, X. Vernede, V. M. Fernandez, E. C. Hatchikian and J. C. Fontecilla-Camps, *J. Am. Chem. Soc.*, 2001, **123**, 1596.
15 O. Pilak, B. Mamat, S. Vogt, C. H. Hagemeier, R. K. Thauer, S. Shima, C. Vonrhein, E. Warkentin and U. Ermler, *J. Mol. Biol.*, 2006, **358**, 798.
16 S. Shima, O. Pilak, S. Vogt, M. Schick, M. S. Stagni, W. Meyer-Klaucke, E. Warkentin, R. K. Thauer and U. Ermler, *Science*, 2008, **321**, 572.
17 T. Hiromoto, K. Ataka, O. Pilak, S. Vogt, M. S. Stagni, W. M. Meyer-Klaucke, E. Warkentin, R. K. Thauer, S. Shima and U. Ermler, *FEBS J.*, 2009, **583**, 585.
18 T. Yagi, *J. Biochem.*, 1970, **68**, 649.
19 N. Yahata, T. Saitoh, Y. Takayama, K. Ozawa, H. Ogata, Y. Higuchi and H. Akutsu, *Biochemistry*, 2006, **45**, 1653.
20 A. J. Pierik, W. Roseboom, R. P. Happe, K. A. Bagley and S. P. J. Albracht, *J. Biol. Chem.*, 1999, **274**, 3331.
21 S. E. Lamle, S. P. J. Albracht and F. A. Armstrong, *J. Am. Chem. Soc.*, 2004, **126**, 14899.
22 H. Ogata, S. Hirota, A. Nakahara, H. Komori, N. Shibata, T. Kato, K. Kano and Y. Higuchi, *Structure*, 2005, **13**, 1635.
23 A. Volbeda, L. Martin, C. Cavazza, M. Matho, B. W. Faber, W. Roseboom, S. P. J. Albracht, E. Garcin, M. Rousset and J. C. Fontecilla-Camps, *J. Biol. Inorg. Chem.*, 2005, **10**, 239.
24 B. Bleijlevens, F. A. van Broekhuizen, A. L. De Lacey, W. Roseboom, V. M. Fernandez and S. P. J. Albracht, *J. Biol. Inorg. Chem.*, 2004, **9**, 743.
25 C. Fichtner, C. Laurich, E. Bothe and W. Lubitz, *Biochemistry*, 2006, **45**, 9706.
26 Y. Montet, P. Amara, A. Volbeda, X. Vernede, E. C. Hatchikian, M. J. Field, M. Frey and J. C. Fontecilla-Camps, *Nat. Struct. Biol.*, 1997, **4**, 523.

27 P. M. Matias, C. M. Soares, L. M. Saraiva, R. Coelho, J. Morais, J. Le Gall and M. A. Carrondo, *J. Biol. Inorg. Chem.*, 2001, **6**, 63.
28 P. Kellers, H. Ogata and W. Lubitz, *Acta Crystallogr., Sect. F: Struct. Biol. Cryst. Commun.*, 2008, **64**, 719.
29 S. E. Lamle, S. P. J. Albracht and F. A. Armstrong, *J. Am. Chem. Soc.*, 2005, **127**, 6595.
30 K. A. Vincent, J. A. Cracknell, A. Parkin and F. A. Armstrong, *Dalton Trans.*, 2005, 3397.
31 M. Bernhard, T. Buhrke, B. Bleijlevens, A. L. De Lacey, V. M. Fernandez, S. P. J. Albracht and B. Friedrich, *J. Biol. Chem.*, 2001, **276**, 15592.
32 M. Carepo, D. L. Tierney, C. D. Brondino, T. C. Yang, A. Pamplona, J. Telser, I. Moura, J. J. G. Moura and B. M. Hoffman, *J. Am. Chem. Soc.*, 2002, **124**, 281.
33 Y. Higuchi and T. Yagi, *Biochem. Biophys. Res. Commun.*, 1999, **255**, 295.
34 K. A. Vincent, N. A. Belsey, W. Lubitz and F. A. Armstrong, *J. Am. Chem. Soc.*, 2006, **128**, 7448.
35 T. Matsumoto, Y. Nakaya and K. Tatsumi, *Organometallics*, 2006, **25**, 4835.
36 T. Matsumoto, Y. Nakaya, N. Itakura and K. Tatsumi, *J. Am. Chem. Soc.*, 2008, **130**, 2458.
37 M. van Gastel, M. Stein, M. Brecht, O. Schröder, F. Lendzian, R. Bittl, H. Ogata, Y. Higuchi and W. Lubitz, *J. Biol. Inorg. Chem.*, 2006, **11**, 41.
38 A. Perra, Q. Wang, A. J. Blake, E. S. Davies, J. McMaster, C. Wilson and M. Schröder, *Dalton Trans.*, 2009, 925.
39 M. van Gastel, C. Fichtner, F. Neese and W. Lubitz, *Biochem. Soc. Trans.*, 2005, **33**, 7.
40 O. Trofanchuk, M. Stein, C. Gessner, F. Lendzian, Y. Higuchi and W. Lubitz, *J. Biol. Inorg. Chem.*, 2000, **5**, 36.
41 M. Flores, A. G. Agrawal, M. van Gastel, W. Gärtner and W. Lubitz, *J. Am. Chem. Soc.*, 2008, **130**, 2402.
42 Y. Higuchi, H. Ogata, K. Miki, N. Yasuoka and T. Yagi, *Structure*, 1999, **7**, 549.
43 M. Brecht, M. van Gastel, T. Buhrke, B. Friedrich and W. Lubitz, *J. Am. Chem. Soc.*, 2003, **125**, 13075.
44 S. Foerster, M. Stein, M. Brecht, H. Ogata, Y. Higuchi and W. Lubitz, *J. Am. Chem. Soc.*, 2003, **125**, 83.
45 S. Foerster, M. van Gastel, M. Brecht and W. Lubitz, *J. Biol. Inorg. Chem.*, 2005, **10**, 51.
46 M. Stein and W. Lubitz, *Phys. Chem. Chem. Phys.*, 2001, **3**, 5115.
47 M. Stein and W. Lubitz, *Phys. Chem. Chem. Phys.*, 2001, **3**, 2668.
48 A. G. Agrawal, M. van Gastel, W. Gärtner and W. Lubitz, *J. Phys. Chem. B*, 2006, **110**, 8142.
49 M. Stein and W. Lubitz, *J. Inorg. Biochem.*, 2004, **98**, 862.
50 M. Medina, R. Williams, R. Cammack and E. C. Hatchikian, *J. Chem. Soc., Faraday Trans.*, 1994, **90**, 2921.
51 F. Dole, M. Medina, C. More, R. Cammack, P. Bertrand and B. Guigliarelli, *Biochemistry*, 1996, **35**, 16399.
52 C. Fichtner, M. van Gastel and W. Lubitz, *Phys. Chem. Chem. Phys.*, 2003, **5**, 5507.
53 J. W. van der Zwaan, J. M. C. C. Coremans, E. C. M. Bouwens and S. P. J. Albracht, *Biochim. Biophys. Acta*, 1990, **1041**, 101.
54 S. J. George, S. Kurkin, R. N. F. Thorneley and S. P. J. Albracht, *Biochemistry*, 2004, **43**, 6808.
55 K. A. Bagley, C. J. Van Garderen, M. Chen, E. C. Duin, S. P. J. Albracht and W. H. Woodruff, *Biochemistry*, 1994, **33**, 9229.
56 H. Ogata, Y. Mizoguchi, N. Mizuno, K. Miki, S. Adachi, N. Yasuoka, T. Yagi, O. Yamauchi, S. Hirota and Y. Higuchi, *J. Am. Chem. Soc.*, 2002, **124**, 11628.
57 S. Dementin, B. Burlat, A. L. De Lacey, A. Pardo, G. Adryanczyk-Perrier, B. Guigliarelli, V. M. Fernandez and M. Rousset, *J. Biol. Chem.*, 2004, **279**, 10508.
58 W. Lubitz, M. van Gastel and W. Gärtner, *Met. Ions Life Sci.*, 2007, **2**, 279.
59 M. Teixeira, I. Moura, A. V. Xavier, J. J. G. Moura, J. Legall, D. V. DerVartanian, H. D. Peck and B. H. Huynh, *J. Biol. Chem.*, 1989, **264**, 16435.
60 M. Brecht, PhD Thesis, Technische Universität, Berlin, 2001.
61 S. P. J. Albracht, M. L. Kalkman and E. C. Slater, *Biochim. Biophys. Acta*, 1983, **724**, 309.
62 R. Bingemann and A. Klein, *Eur. J. Biochem.*, 2000, **267**, 6612.
63 M. Rousset, Y. Montet, B. Guigliarelli, N. Forget, M. Asso, P. Bertrand, J. C. Fontecilla-Camps and E. C. Hatchikian, *Proc. Natl. Acad. Sci. U. S. A.*, 1998, **95**, 11625.
64 V. H. Teixeira, C. M. Soares and A. M. Baptista, *Proteins: Struct. Funct. Bioinf.*, 2008, **70**, 1010.
65 I. F. Galvan, A. Volbeda, J. C. Fontecilla-Camps and M. J. Field, *Proteins: Struct. Funct. Bioinf.*, 2008, **73**, 195.
66 T. Yagi, M. Tsuda and H. Inokuchi, *J. Biochem.*, 1973, **73**, 1069.
67 K. A. Vincent, J. A. Cracknell, O. Lenz, I. Zebger, B. Friedrich and F. A. Armstrong, *Proc. Natl. Acad. Sci. U. S. A.*, 2005, **102**, 16951.
68 T. Buhrke, O. Lenz, N. Krauss and B. Friedrich, *J. Biol. Chem.*, 2005, **280**, 23791.
69 M. Ludwig, J. A. Cracknell, K. A. Vincent, F. A. Armstrong and O. Lenz, *J. Biol. Chem.*, 2009, **284**, 465.
70 F. Leroux, S. Dementin, B. Burlat, L. Cournac, A. Volbeda, S. Champ, L. Martin, B. Guigliarelli, P. Bertrand, J. Fontecilla-Camps, M. Rousset and C. Leger, *Proc. Natl. Acad. Sci. U. S. A.*, 2008, **105**, 11188.
71 F. A. Armstrong, N. A. Belsey, J. A. Cracknell, G. Goldet, A. Parkin, E. Reisner, K. A. Vincent and A. F. Wait, *Chem. Soc. Rev.*, 2009, **38**, 36.
72 B. Bleijlevens, T. Buhrke, E. van der Linden, B. Friedrich and S. P. J. Albracht, *J. Biol. Chem.*, 2004, **279**, 46686.
73 T. Burgdorf, O. Lenz, T. Buhrke, E. van der Linden, A. K. Jones, S. P. J. Albracht and B. Friedrich, *J. Mol. Microbiol. Biotechnol.*, 2005, **10**, 181.
74 K. A. Vincent, A. Parkin, O. Lenz, S. P. J. Albracht, J. C. Fontecilla-Camps, R. Cammack, B. Friedrich and F. A. Armstrong, *J. Am. Chem. Soc.*, 2005, **127**, 18179.
75 F. Osterloh, W. Saak, D. Haase and S. Pohl, *Chem. Commun.*, 1997, 979.
76 S. C. Davies, D. J. Evans, D. L. Hughes, S. Longhurst and J. R. Sanders, *Chem. Commun.*, 1999, 1935.
77 W. F. Liaw, C. Y. Chiang, G. H. Lee, S. M. Peng, C. H. Lai and M. Y. Darensbourg, *Inorg. Chem.*, 2000, **39**, 480.
78 M. A. Reynolds, T. B. Rauchfuss and S. R. Wilson, *Organometallics*, 2003, **22**, 1619.
79 Z. L. Li, Y. Ohki and K. Tatsumi, *J. Am. Chem. Soc.*, 2005, **127**, 8950.
80 Y. Oudart, V. Artero, J. Pecaut and M. Fontecave, *Inorg. Chem.*, 2006, **45**, 4334.
81 A. D. Wilson, R. K. Shoemaker, A. Miedaner, J. T. Muckerman, D. L. Dubois and M. R. Dubois, *Proc. Natl. Acad. Sci. U. S. A.*, 2007, **104**, 6951.
82 Y. Oudart, V. Artero, J. Pecaut, C. Lebrun and M. Fontecave, *Eur. J. Inorg. Chem.*, 2007, 2613.
83 A. D. Wilson, K. Fraze, B. Twamley, S. M. Miller, D. L. Dubois and M. R. Dubois, *J. Am. Chem. Soc.*, 2008, **130**, 1061.
84 M. van Gastel, J. L. Shaw, A. J. Blake, M. Flores, M. Schröder, J. McMaster and W. Lubitz, *Inorg. Chem.*, 2008, **47**, 11688.
85 S. Ogo, R. Kabe, K. Uehara, B. Kure, T. Nishimura, S. C. Menon, R. Harada, S. Fukuzumi, Y. Higuchi, T. Ohhara, T. Tamada and R. Kuroki, *Science*, 2007, **316**, 585.
86 B. Kure, T. Matsumoto, K. Ichikawa, S. Fukuzumi, Y. Higuchi, T. Yagi and S. Ogo, *Dalton Trans.*, 2008, 4747.
87 T. Matsumoto, B. Kure and S. Ogo, *Chem. Lett.*, 2008, **37**, 970.
88 M. Bruschi, G. Zampella, P. Fantucci and L. De Gioia, *Coord. Chem. Rev.*, 2005, **249**, 1620.
89 A. Pardo, A. L. De Lacey, V. M. Fernandez, H. J. Fan, Y. B. Fan and M. B. Hall, *J. Biol. Inorg. Chem.*, 2006, **11**, 286.
90 A. Volbeda and J. C. Fontecilla-Camps, *Top. Organomet. Chem.*, 2006, **17**, 57.
91 W. Lubitz, E. J. Reijerse and J. Messinger, *Energy Environ. Sci.*, 2008, **1**, 15.
92 Y. Higuchi, F. Toujou, K. Tsukamoto and T. Yagi, *J. Inorg. Biochem.*, 2000, **80**, 205.